

The human DNA methyltransferases (DNMTs) 1, 3a and 3b: coordinate mRNA expression in normal tissues and overexpression in tumors

Keith D. Robertson, Eva Uzvolgyi¹, Gangning Liang, Cathy Talmadge², Janos Sumegi², Felicidad A. Gonzales and Peter A. Jones*

University of Southern California, Norris Comprehensive Cancer Center, MS 83, 1441 Eastlake Avenue, Los Angeles, CA 90033, USA and ¹Room 4027, Wittson Hall and ²Room 102, UGC, University of Nebraska Medical Center, Department of Pathology, 600 South and 42nd Street, Omaha, NB 68198, USA

Received February 24, 1999; Revised and Accepted April 12, 1999

DDBJ/EMBL/GenBank accession nos AF129267–AF129269

ABSTRACT

DNA methylation in mammals is required for embryonic development, X chromosome inactivation and imprinting. Previous studies have shown that methylation patterns become abnormal in malignant cells and may contribute to tumorigenesis by improper *de novo* methylation and silencing of the promoters for growth-regulatory genes. RNA and protein levels of the DNA methyltransferase *DNMT1* have been shown to be elevated in tumors, however murine stem cells lacking *Dnmt1* are still able to *de novo* methylate viral DNA. The recent cloning of a new family of DNA methyltransferases (*Dnmt3a* and *Dnmt3b*) in mouse which methylate hemimethylated and unmethylated templates with equal efficiencies make them candidates for the long sought *de novo* methyltransferases. We have investigated the expression of human *DNMT1*, *3a* and *3b* and found widespread, coordinate expression of all three transcripts in most normal tissues. Chromosomal mapping placed *DNMT3a* on chromosome 2p23 and *DNMT3b* on chromosome 20q11.2. Significant overexpression of *DNMT3b* was seen in tumors while *DNMT1* and *DNMT3a* were only modestly overexpressed and with lower frequency. Lastly, several novel alternatively spliced forms of *DNMT3b*, which may have altered enzymatic activity, were found to be expressed in a tissue-specific manner.

INTRODUCTION

Mammalian cells possess the capacity to epigenetically modify their genomes via DNA methylation. Methylation occurs at the 5 position of the cytosine ring within the context of the CpG dinucleotide (1). Approximately 70% of the CpG residues in the mammalian genome are methylated, however the distribution of CpG is not random and the majority of the genome is CpG-poor (2). Certain regions of the genome which are often, but not

always, clustered at the 5'-ends of genes possess the expected CpG frequency and have been termed CpG islands (3). CpG islands are not normally methylated in cells and the mechanism preventing islands from becoming *de novo* methylated may involve transcription factor binding (4,5). The effects of DNA methylation on cells include transcriptional repression by methylation of promoter regions (6), formation of compact chromatin structures (7), X chromosome inactivation (8) and imprinting control (9).

Until recently only one DNA methyltransferase, *DNMT1*, had been cloned from human and mouse cells. *DNMT1* is a large enzyme (193.5 kDa) composed of a C-terminal catalytic domain with homology to bacterial cytosine 5-methylases and a large N-terminal regulatory domain with several functions, including targeting to replication foci (10–13). Disruption of *Dnmt1* in mice results in abnormal imprinting (9), embryonic lethality, greatly reduced levels of DNA methylation (14) and derepression of endogenous retroviruses (15). *Dnmt1*^{-/-} embryonic stem (ES) cells are viable and still possess the ability to *de novo* methylate viral DNA, suggesting the existence of an independently encoded *de novo* DNA methyltransferase (16).

Several forms of *DNMT1* have been detected which differ in their translation start sites and their preferences for hemimethylated versus unmethylated substrates (17). Targeting of *DNMT1* to replication foci via the N-terminal domain is believed to allow for copying of methylation patterns from the parental to the newly synthesized daughter DNA strand. Forced overexpression of *DNMT1* or cleavage between the N-terminal regulatory domain and C-terminal catalytic domain has been shown to result in increased *de novo* methylation activity (18,19) and cellular transformation (20). *DNMT1* RNA and activity levels were shown to be elevated in colon cancer relative to adjacent normal mucosa and this was proposed to be responsible for the abnormal methylation patterns observed in this and other tumor types (21–23). Another study, however, showed only very small increases in *DNMT1* RNA when the proliferative status of the tumor and normal tissue was taken into account, calling into

*To whom correspondence should be addressed. Tel: +1 323 865 0816; Fax: +1 323 865 0102; Email: jones_p@froggy.hsc.usc.edu

question the exact role of *DNMT1* overexpression in tumorigenesis (24).

Since *de novo* methylation activity remains in *Dnmt1* knockout ES cells and because the exact role of *DNMT1* in tumor-specific methylation abnormalities remains unclear, a search for additional DNA methyltransferases was carried out by several groups. A second potential DNA methyltransferase, *Dnmt2*, was isolated by two groups but has not been shown to possess methylation ability (25,26). Recently another group of DNA methyltransferases, *DNMT3a* and *3b*, was isolated by database search. These related enzymes were shown to be expressed at increased levels in undifferentiated ES cells and were down-regulated in differentiating ES cells and adult murine tissues. Furthermore, both *Dnmt3a* and *3b* methylated hemimethylated and unmethylated DNA with equal efficiencies, making them potential candidates for the long sought *de novo* methyltransferases (27). In the present work we have investigated the expression patterns of human *DNMT1*, *DNMT3a* and *DNMT3b* in normal and tumor tissues. We found high level expression of all three transcripts in a coordinate manner in most fetal tissues examined and lower level, but still widespread, expression in most adult tissues. Analysis of expression levels in tumor and adjacent normal tissues showed that *DNMT1* and *3a* were overexpressed (at >2-fold) at low frequency, while *DNMT3b* was overexpressed at higher frequency even when the proliferative status of the tumor was taken into account. Furthermore, several novel splice variants of *DNMT3b* were detected and characterized which have the potential to alter its catalytic activity.

MATERIALS AND METHODS

GenBank accession numbers

The cDNA sequences of the human *DNMT3b* splice variants have been deposited in GenBank under accession nos AF129267 for *DNMT3b1*, AF129268 for *DNMT3b4* and AF129269 for *DNMT3b5*.

Human tissues and RNA preparation

Normal human tissue cDNA preparations were purchased from Clontech. Bladder, colon, kidney and pancreas tumor and adjacent normal tissues were collected at the USC/Norris Comprehensive Cancer Hospital in accordance with institutional guidelines and immediately frozen in liquid nitrogen. RNA was extracted as described previously (28).

Reverse transcriptase (RT)-PCR

Reverse transcription was carried out with random hexamers (Pharmacia), Superscript II reverse transcriptase (Life Technologies) and 2.5 µg of total RNA as recommended by the manufacturer and as described previously (28) in a total volume of 50 µl. One microliter of RT reaction was used for subsequent PCR amplification for each of the desired transcripts with dNTPs (Boehringer Mannheim) and *Taq* DNA polymerase (Sigma) as described (29). Primer sequences used were as follows: *DNMT3a* sense, 5'-GGG GAC GTC CGC AGC GTC ACA C-3'; *DNMT3a* antisense, 5'-CAG GGT TGG ACT CGA GAA ATC GC-3'; *DNMT3b* sense, 5'-CCT GCT GAA TTA CTC ACG CCC C-3'; *DNMT3b* antisense, 5'-GTC TGT GTA GTG CAC AGG AAA GCC-3'; *DNMT1* sense, 5'-GAT CGA ATT CAT GCC GGC

GCG TAC CGC CCC AG-3'; *DNMT1* antisense, 5'-ATG GTG GTT TGC CTG GTG C-3'; β-actin sense, 5'-GGA GTC CTG TGG CAT CCA CG-3'; β-actin antisense, 5'-CTA GAA GCA TTT GCG GTG GA-3'. The proliferating cell nuclear antigen (PCNA) primers, probe and amplification conditions have been described previously (29). Amplification conditions were: 94°C for 2.0 min, 1 cycle, 94°C for 0.5 min, transcript-specific annealing temperature for 1.0 min, and 72°C for 1.0 min for a cycle number optimized for each set of primers and RNA sample to keep amplification within the linear range. Annealing temperatures were 65°C for *DNMT3a* and *3b*, 58°C for *DNMT1* and 60°C for β-actin. Cycle numbers varied between 18 and 25 for β-actin, 25 and 30 for PCNA and 30 and 35 for the DNMT transcripts. Generally the RNA derived from the tumor and adjacent normal tissues required a higher number of cycles compared to the commercially available normal tissue samples. PCR reactions were electrophoresed on 1.5% agarose gels, transferred to nylon membrane (Genescreen Plus; NEN) and hybridized to end-labeled oligonucleotide probes at 48°C as described previously (29). Probe sequences were as follows: *DNMT3a*, 5'-CCG CGC ATC ATG CAG GAG GCG GTA GAA CTC-3'; *DNMT3b*, 5'-CAC TGG ATT ACA CTC CAG GAA CCG TGA GAT G-3'; *DNMT1*, 5'-ATG GCA GAT GCC AAC AGC CC-3'; β-actin, 5'-ACA TCC GCA AAG ACC TGT ACG CCA ACA CAG-3'.

Northern blot analysis

The fetal tissue northern blot was purchased from Invitrogen and the human adult northern blot was purchased from Clontech. Probes were labeled with the Random-Prime DNA Label Kit (Boehringer Mannheim) and hybridized at 65°C in ExpressHyb hybridization buffer (Clontech) according to the manufacturer's instructions. The *DNMT3a* cDNA probe corresponded to the *EcoRI*-*NcoI* fragment (376 bp) derived from the EST plasmid containing the *DNMT3a* cDNA (GenBank accession no. W76111) and the *DNMT3b* cDNA probe corresponded to the *HindIII*-*SmaI* fragment (324 bp) derived from the EST plasmid containing the *DNMT3b3* cDNA (GenBank accession no. T66356) (27). The *DNMT1* probe corresponded to the *EcoRI*-*XbaI* fragment (330 bp) derived from plasmid pKR11D-6. pKR11D-6 was created by RT-PCR with Raji cell line RNA as template and primers sense, 5'-GAT CGA ATT CAT GCC GGC GCG TAC CGC CCC AG-3', and antisense, 5'-ACA CAG GTG ACC GTG CTT ACA GTA CAC-3', and PCR conditions identical to those described above for *DNMT1*, except an extension time of 3 min was used. The 1249 bp band generated (corresponding to bp 1-1249 of human *DNMT1*; 30) was cloned with the T7Blue-Blunt cloning system (Novagen) and sequenced. For β-actin, an end-labeled oligonucleotide probe was used (5'-CTG TGT TGG CGT ACA GGT CTT TGC GGA TGT-3') and the hybridization conditions were identical except the temperature was lowered to 48°C.

Cloning and analysis of *DNMT3b* splice variants

The four RT-PCR products generated after amplification of human testis cDNA with *DNMT3b* primers were separated on a 1.5% agarose gel then each fragment was gel purified using the Qiaex II gel extraction kit (Qiagen) according to the manufacturer's instructions and cloned using the T7Blue-Blunt cloning kit (Novagen). At least two independent clones corresponding to

each transcript were isolated and sequenced at the USC Microchemical Core Facility and aligned with the EST sequence for human *DNMT3b3* (GenBank accession no. T66356) and murine *Dnmt3b1* cDNA (GenBank accession no. AF068626) (27). Human testis cDNA was used as template because it was the only tissue we examined which expressed significant levels of all four splice variants.

Chromosomal mapping

Fluorescence *in situ* hybridization (FISH) was carried out on normal female lymphocyte chromosome spreads as described previously (31). Probes for *DNMT3a* and *DNMT3b*, which corresponded to the entire cDNA inserts derived from the respective EST plasmids (GenBank accession nos W76111 and T66356 for *DNMT3a* and *3b*, respectively) were labeled with biotin, hybridized to chromosome spreads, r-banded and then detected with fluorescein-avidin.

RESULTS

DNMT1, *3a* and *3b* are coordinately expressed in most human tissues

Northern blotting with poly(A)-selected RNA was initially employed to quantitatively examine DNMT expression levels in a panel of fetal and adult human tissues. Transcripts for *DNMT3a* (Fig. 1A) and *DNMT1* (Fig. 1C) were present at high levels in all fetal tissues examined while *DNMT3b* (Fig. 1B) was expressed at high levels only in fetal liver. *DNMT3b* transcripts were detectable after long exposure in all fetal tissues (not shown). It is interesting to note that fetal liver expressed extremely high levels of all DNMTs, which may be due to residual hematopoiesis in this tissue (32). Transcripts for *DNMT3a* and *3b* were readily detectable in adult heart, skeletal muscle, thymus, kidney, liver, placenta and peripheral blood mononuclear cells (PBMC) and appeared to be coordinately expressed in many cases (Fig. 1). Bands were detectable in all tissues after long exposure (not shown). *DNMT3a* and *3b* transcripts were slightly larger than the previously reported murine homologs (27). *DNMT1* was expressed at detectable levels in all adult tissues except small intestine. It is also notable that multiple bands hybridized in many tissues for all three transcripts, but especially *DNMT3a* and *3b*, and is most likely due to alternative splicing, as will be discussed next and has been noted previously for *DNMT1* (33,34). Hybridization with a β -actin probe (Fig. 1D) indicated that samples were of good quality and equally loaded. Based on exposure times for each blot, a similar probe size and ^{32}P incorporation efficiency, the approximate levels of each DNMT in a given tissue can be ordered as follows: *DNMT1* (overnight exposure) > *DNMT3a* (1–3 days exposure) > *DNMT3b* (10 days exposure). A quantitative comparison of the RNA levels of each DNMT in a tissue present in both the fetal and adult northern blots (liver), which takes into account both phosphorimager quantitation and exposure times, is shown in Figure 1E. These results indicate that *DNMT1* is the predominant DNMT in all tissues.

DNMT3a and *DNMT3b* possess significant homology which could result in cross-hybridization in the northern analysis (note that there was no homology between the N-terminal *DNMT1* probe used here and *DNMT3a* or *3b*). We think this is unlikely to be the reason we observe coordinate expression of *DNMT3a* and *3b* for several reasons. The first is that high levels of *DNMT3a*

were detectable in all fetal tissues while *DNMT3b* was only detected at high levels in fetal liver. If the *DNMT3b* probe cross-hybridized even poorly with *DNMT3a* then the differences seen in Figure 1A and B should be far less pronounced, especially since the *DNMT3b* blot was exposed for a longer period of time. Second, northern analysis of MCF7 breast cancer cells following synchronization and release showed readily detectable differences in the expression of *DNMT3a* and *3b* (data not shown). To further examine the degree of coordinate expression of the three DNMTs, semi-quantitative RT-PCR with independently prepared RNA samples representing a subset of the tissues analyzed in Figure 1 followed by hybridization and quantitation was carried out. Primers employed for this analysis were 100% specific for each DNMT transcript (data not shown). Figure 2 shows that the three DNMTs were coordinately expressed in most tissues, with the exception of skeletal muscle which showed similar differences in the northern blot analysis as well. The absolute levels of each DNMT by RT-PCR analysis paralleled the northern hybridization intensities in many cases (brain, heart, skeletal muscle, colon, spleen and placenta for example) but not all (liver and PBMC for example) and is most likely due to the semi-quantitative nature of the RT-PCR analysis and differences in origin and preparation of the RNA samples.

Alternative splicing in the 3'-end of *DNMT3b*

Several splice variants of murine *DNMT3b* have been previously reported. One of these regions was within the C-terminal catalytic domain and thus had the potential to alter catalytic activity (27). Such splice variants, some of which delete the catalytic site (conserved methyltransferase motif IV) and alter the spacing between motifs, have been reported for *DNMT1* (33). We used semi-quantitative RT-PCR to examine potential *DNMT3b* splice variants in a panel of 13 normal human tissues followed by Southern hybridization with an internal oligonucleotide probe. Figure 3A shows that expression of multiple *DNMT3b* variants could be detected in all tissues examined. Amplification of PCNA (Fig. 3B) and β -actin (Fig. 3C) served as controls for proliferative state and RNA integrity, respectively. PCNA levels were elevated in 'proliferating tissues' such as the small intestine, testis, placenta and colon (Fig. 3B). A total of four *DNMT3b* bands could be detected in human testis DNA and each band was cloned and sequenced. The structures of the four splice variants are shown schematically in Figure 4A (top) with their migration in the agarose gel shown in Figure 4A (bottom). The predicted protein products are aligned with the murine *Dnmt3b1* sequence (27) in Figure 4B. Two of the four transcripts correspond to previously described splice variants of murine *Dnmt3b* (*Dnmt3b1* and *3b3*) while two others are novel (termed *DNMT3b4* and *3b5* in Fig. 4). These latter two transcripts give rise to truncated protein products due to frameshifts after splicing resulting in loss of the conserved methyltransferase motifs IX and X (11). *DNMT3b4* terminates one amino acid after the splice junction (a deletion of 108 amino acids relative to *DNMT3b1*), while *DNMT3b5* encodes a novel 45 amino acid region followed by a stop codon (Fig. 4B). It can be seen in Figure 3A that *DNMT3b3* (lowest band) was ubiquitously expressed in normal tissues while *DNMT3b1* (top band) was expressed in all tissues except brain, skeletal muscle and PBMC. *DNMT3b4* (upper middle band) was expressed in all tissues except brain, skeletal muscle, lung and prostate while *DNMT3b5* (lower middle band) was detectable

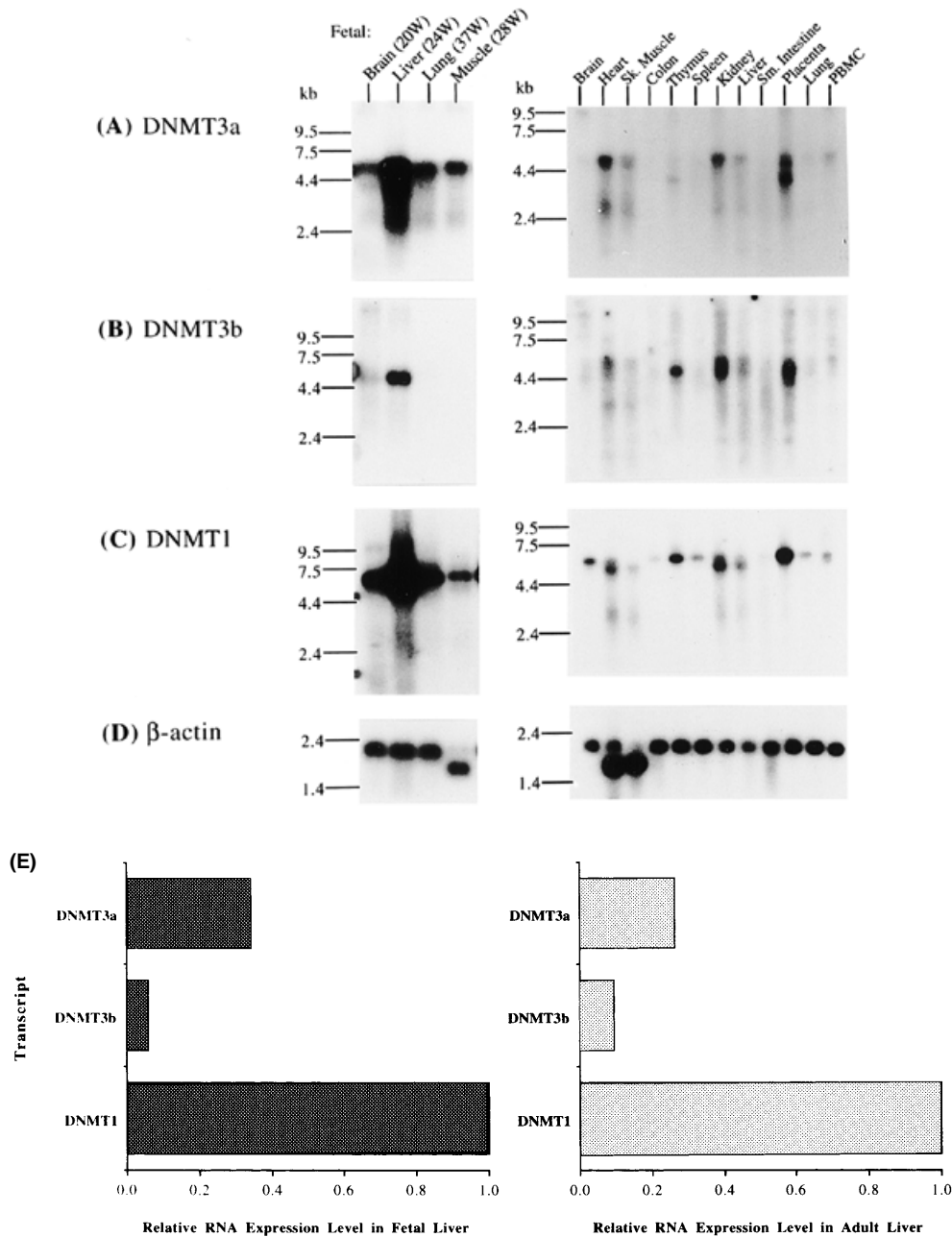


Figure 1. Northern analysis of expression levels of DNMTs in normal human tissues. Approximately 2 μ g of poly(A)-selected RNA derived from fetal tissues (left), with age given in weeks at the top, or adult tissues (right) was hybridized to cDNA probes specific for (A) *DNMT3a*, (B) *DNMT3b* and (C) *DNMT1*. β -Actin (D) served as a control for RNA integrity and indicated that samples were equally loaded. Molecular weights in kilobases (kb) are indicated at the left of each panel. PBMC, peripheral blood mononuclear cell; Sm. int., small intestine; Sk. muscle, skeletal muscle. (E) Summary of the relative levels of each DNMT in fetal and adult liver derived from phosphorimager quantitation of results in (A)–(C) and exposure times. This tissue was used since it expressed relatively high levels of all DNMTs making quantitation more accurate and because it was a tissue present on both the fetal and adult northern blots. Results are expressed relative to the *DNMT1* level on each blot (set at 1.0). Note, however, that expression levels in fetal liver were nearly 20-fold higher than in adult liver.

only in testis and at a very low level in brain and prostate (Fig. 3A). It should also be noted that the additional *Dnmt3b* splice variant (*Dnmt3b2*) described in murine tissues could not be distinguished from *DNMT3b1* in our analysis because the *Dnmt3b2* alternatively spliced region was located 5' to our RT-PCR primers (27).

Chromosomal mapping of *DNMT3a* and *3b*

Given that *DNMT3a* and *3b* appeared to be coordinately expressed in many tissues we wished to map their chromosomal location. FISH using cDNA probes for each methyltransferase was carried out on normal lymphocyte chromosome spreads and

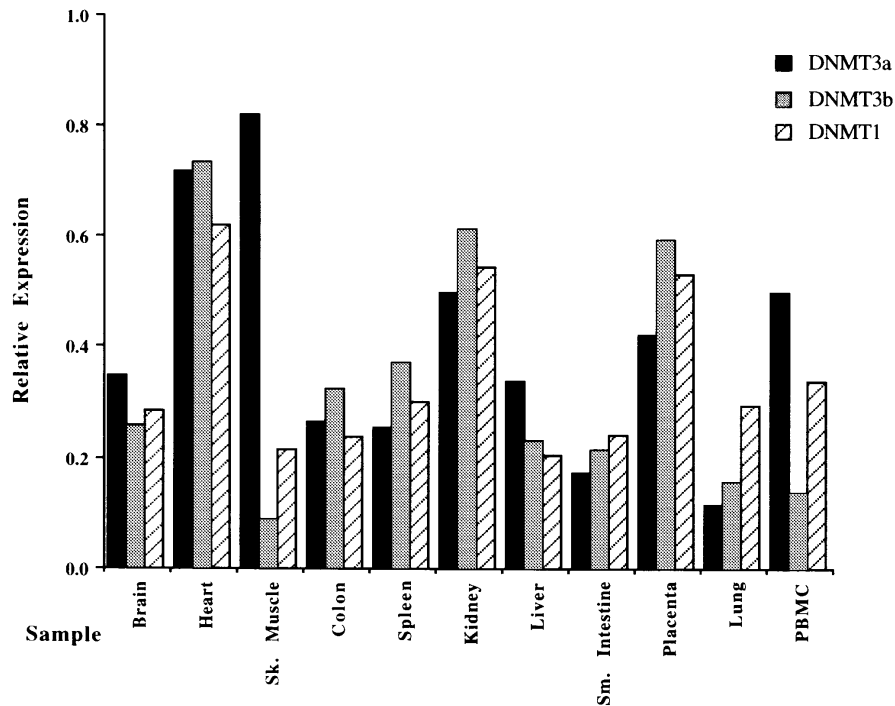


Figure 2. Analysis of DNMT expression levels by semi-quantitative RT-PCR. Primers specific for each DNMT were used with cDNA derived from each of the normal human tissues (Clontech) listed below the graph. These cDNA samples were prepared from different RNA sources than those used for the northern analysis in Figure 1. PCR products were hybridized with internal oligonucleotide probes (not shown), quantitated and expressed relative to β -actin, as a control for RNA integrity. Abbreviations are as in Figure 1.

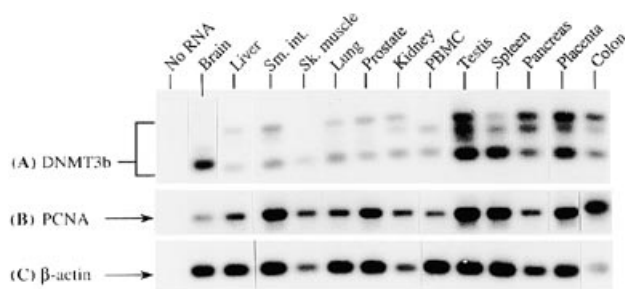


Figure 3. Alternative splicing in the catalytic domain of *DNMT3b* (A) was monitored by RT-PCR using cDNA derived from the normal human tissues (Clontech) indicated above the figure. Amplification of PCNA (B) and β -actin (C) served as controls for proliferative state and RNA integrity, respectively. PCR products were then hybridized to internal oligonucleotide probes specific for each transcript. Abbreviations are as in Figure 1.

indicated that *DNMT3a* was located at chromosome 2p23 and *DNMT3b* was located at chromosome 20q11.2 (data not shown). *DNMT1* has been previously mapped to human chromosome 19p13.2–p13.3 (30).

Overexpression of DNMTs in tumor tissues

Previous studies have revealed significant overexpression of *DNMT1* in tumor tissues (21,22) while another study found very little increase (24). We examined the expression levels of all three methyltransferase genes by RT-PCR from 10 normal-tumor matched sets (five bladder, three colon, one kidney and one

pancreas) and related this to the proliferation-associated marker PCNA. PCNA is a component of the DNA replication apparatus and is also known as the polymerase processivity factor or sliding clamp (35). While its levels vary modestly (3–7-fold depending on the study) during the G₁ to S transition, it is nearly undetectable in G₀ cells by northern blot and its synthesis has been shown to correlate directly with the proliferative state of the cell (36,37). A representative subset of the RT-PCR data from the 10 normal-tumor matched sets for *DNMT1*, *3a* and *3b* is shown in Figure 5. Amplification of PCNA and β -actin served as controls for cell proliferation and sample quality, respectively (Fig. 5). Figure 6 summarizes the fold change (tumor/normal) for the 10 normal-tumor matched sets relative to PCNA for *DNMT3a* (top), *DNMT3b* (middle) and *DNMT1* (bottom). A level of overexpression ≥ 2 -fold was observed in 5 of 10 samples for *DNMT3a*, 6 of 10 samples for *DNMT1* and 8 of 10 samples for *DNMT3b*. *DNMT3b* clearly showed the largest fold increases (an average of 7.5-fold) of all three enzymes and there were several tumors which overexpressed all three enzymes simultaneously, such as bladder sample 16. Levels of overexpression of *DNMT3a* (an average of 3.1-fold) and *DNMT1* (an average of 4.0-fold) were more modest in the majority of the samples, in keeping with a previous study of *DNMT1* (24).

DISCUSSION

In the present paper we have described the expression patterns of the three known, catalytically active DNA methyltransferases in a large number of human fetal and adult tissues and mapped their chromosomal locations. Expression of *DNMT1*, *3a* and *3b* mRNA was widespread in a coordinate manner in most tissues

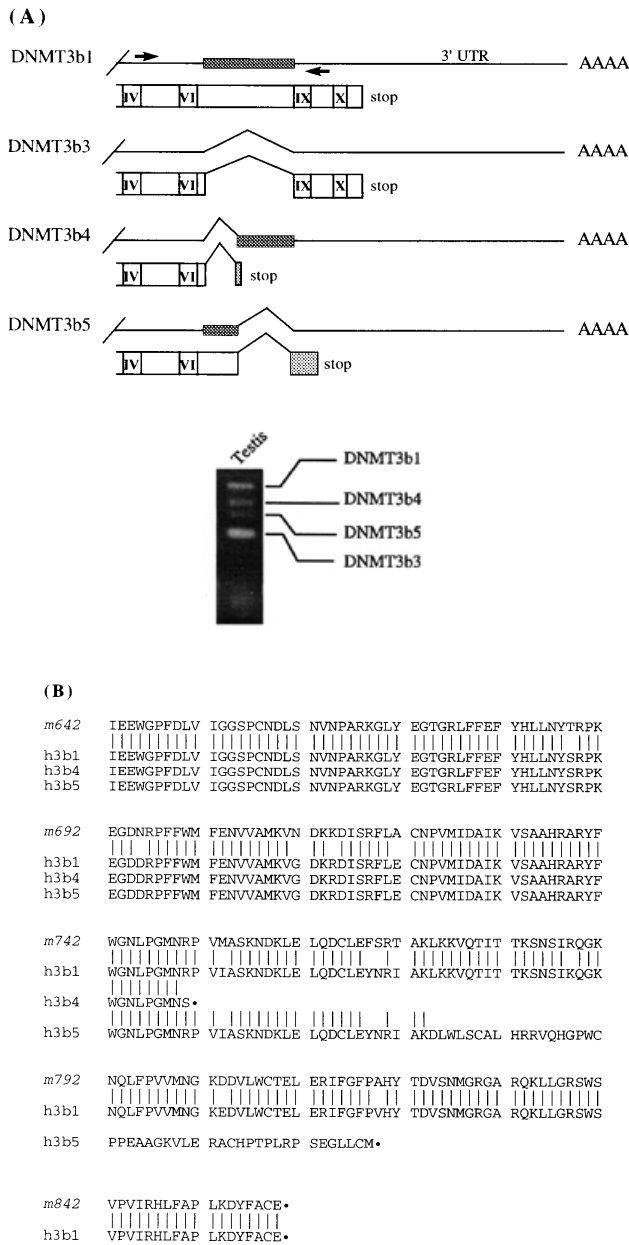


Figure 4. Analysis of 3'-end splice variants of *DNMT3b*. Four splice variants were detected during RT-PCR for *DNMT3b* in normal human testis and a subset of these four were detected in all tissues examined (Fig. 3A). (A) RNA structure (top line, with shaded box indicating the alternatively spliced region) and protein structure (bottom boxes, with white representing unaltered reading frame and shading representing frameshifts) of the four products after cloning and sequence analysis. *DNMT3b1* and *3b3* were similar to the previously reported murine homologs (27), while *DNMT3b4* and *3b5* have not been previously reported. Approximate positions of the most conserved DNA methyltransferase motifs are boxed (11). Arrows represent the locations of the RT-PCR primers. The bottom panel is a representative ethidium bromide stained 1.5% agarose gel showing the migration of each of the splice variants after RT-PCR amplification from human testis RNA. (B) Amino acid sequence alignment of the 3'-ends of human *DNMT3b1*, 4 and 5 alternative splice products with murine *Dnmt3b1* (GenBank accession no. AF068626). Amino acid numbers (in italics) are derived from the previously published murine *Dnmt3b1* sequence (27). Black dots represent stop codons; vertical bars represent identity.

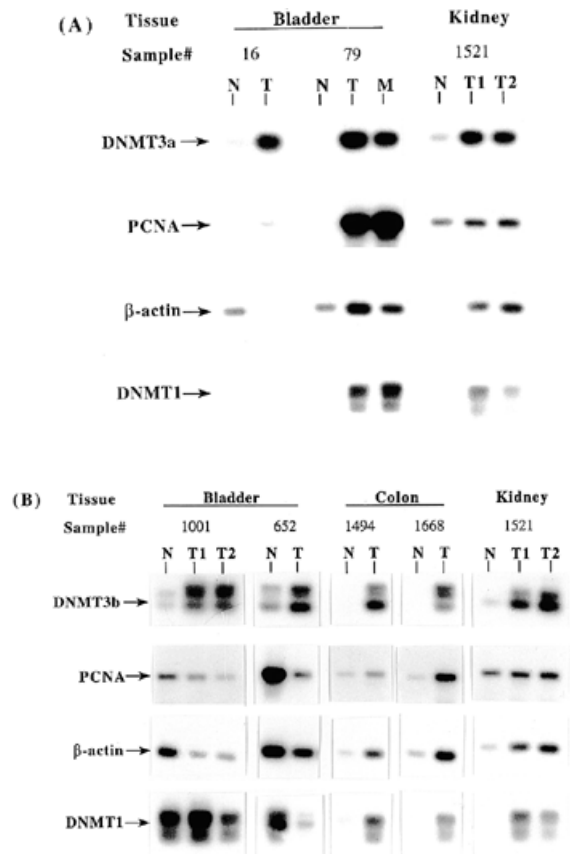


Figure 5. Analysis of DNMT levels in tumor versus normal adjacent tissue. Representative RT-PCR analysis of matched tumor and normal specimens for (A) *DNMT3a* and (B) *DNMT3b*. The tissue source is indicated above. N, normal adjacent tissue; T1, tumor tissue; T2, sample taken from a different region of the same tumor as T1; M, a metastasis. Also shown is RT-PCR amplification of PCNA and β-actin which act as controls for proliferative state and RNA integrity, respectively, and *DNMT1*. RT-PCR products were hybridized to internal oligonucleotide probes specific for each transcript. Note that bladder sample 79 exemplifies a tumor with no significant change in DNMT levels when expressed relative to PCNA (see also Fig. 6). The additional hybridizing band in the *DNMT1* amplifications appeared to be non-specific because it was not observed in all samples (not shown) and was more frequent with the higher cycle numbers required for some of our normal-tumor matched sets.

examined at levels significant enough to be detected by northern blotting. Four splice variants of *DNMT3b* were detected, of which two had been previously reported and two were novel variants. All forms were expressed in a tissue-specific manner and the two novel variants may have altered catalytic activities due to the deletion of two conserved methyltransferase motifs. Significant overexpression of *DNMT3b* was observed in tumor tissues while overexpression of *DNMT1* and *3a* was more modest and was observed in fewer samples.

While there is little doubt that DNA methylation patterns are abnormal in tumor tissues (6,23) there is a question as to the role of *DNMT1* in this process. Several studies have shown high level overexpression of *DNMT1* in colon tumors and forced overexpression of *DNMT1* results in transformation and *de novo* methylation of CpG islands (19,20,22). We found a very modest degree of overexpression of *DNMT1* and *3a* (2-fold in most cases) that is similar to that reported by Lee *et al.* for *DNMT1* (24). Previous studies have indeed shown that murine *Dnmt1* levels vary during the

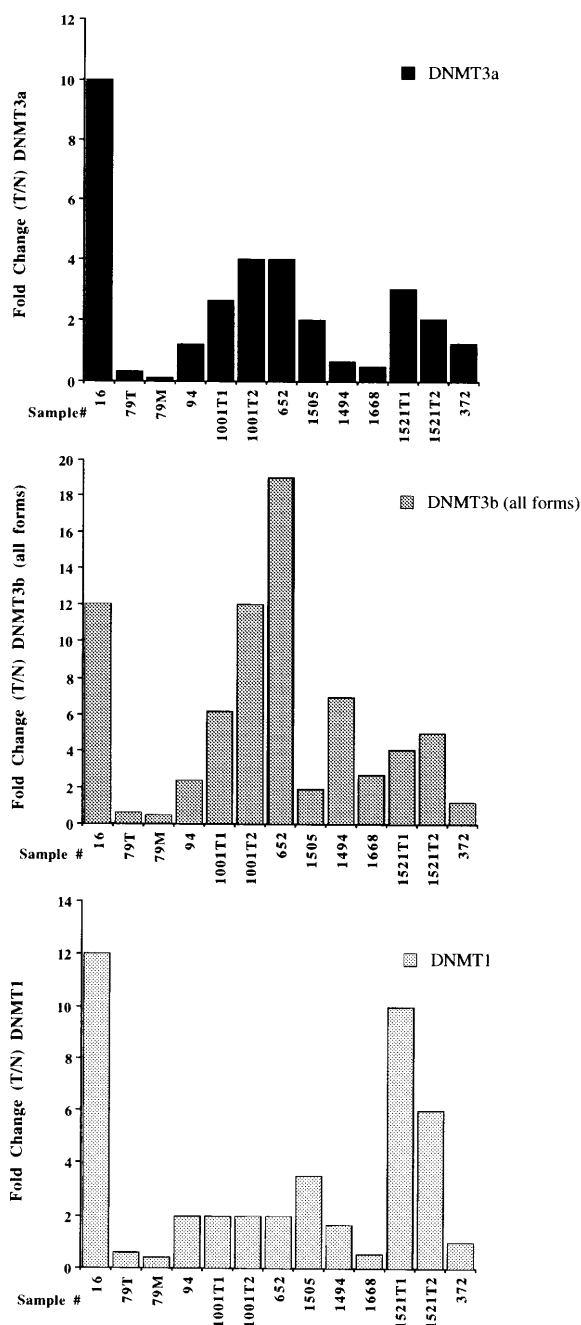


Figure 6. Quantitation of the relative levels of *DNMT3a* (top), *DNMT3b* (middle) and *DNMT1* (bottom) in 10 tumor (T)–normal (N) matched sets. The seven samples shown in Figure 5 and three others (not shown) were quantitated, normalized to β -actin as a control for RNA integrity and set relative to the proliferation-associated transcript PCNA to control for increased cell proliferation in tumor samples. Results are expressed as the fold change, tumor/normal sample. Samples 16, 79 (2), 94, 1001 (2) and 652 were derived from bladder; 1505, 1494 and 1668 were derived from colon; 1521(2) was derived from kidney; and 372 was derived from pancreas. Abbreviations are as in Figure 5.

cell cycle and correlate with cell proliferation (24,38). Overexpression of *DNMT3b* was more frequent and the degree of overexpression significantly higher even when expressed relative to a marker tightly associated with cell proliferation (PCNA). Previous studies have used histone H4 as a marker of proliferation; however, the

induction of expression of PCNA and histone H4 when cells exit G_0 and begin cycling is almost identical and thus we feel both transcripts are acceptable markers of the higher degree of cell proliferation associated with tumors (36).

Are *DNMT3a* and *3b* relevant to cancer? This is a complicated question but our results suggest that they may indeed play a role. While overexpression levels of *DNMT1* and *3a* were modest, *DNMT3b* was significantly overexpressed in most tumors we examined. That *DNMT3a* and *3b* may be involved in the abnormal *de novo* methylation observed in tumors is strengthened by the previous work in ES cells. Undifferentiated ES cells clearly have the capacity to *de novo* methylate DNA (16), like tumor cells, and levels of both *DNMT3a* and *3b* are very high in ES cells (27). Furthermore, amplifications of human chromosome 2p23, the location of *DNMT3a*, are frequent in certain B cell neoplasms (39) and neuroblastomas (40). This region also contains the *N-myc* proto-oncogene (39) and the anaplastic lymphoma kinase gene *ALK* (41). Deletions of portions of the long arm of human chromosome 20, which include the *DNMT3b* locus at 20q11.2, have been reported in a wide spectrum of myeloid disorders (42,43). These tumors will be particularly interesting to examine in terms of their methylation patterns and might provide information as to the exact role of *DNMT3a* and *3b* in cancer.

An interesting aspect of *DNMT3b* was the finding of multiple alternatively spliced forms. Four forms, arising from alternative splicing near the 3'-end, were expressed in a tissue-specific manner and several of these forms were up-regulated in tumors more frequently than others. *DNMT3b3* was ubiquitously expressed in normal tissues and most tumors and possesses the conserved methyltransferase motifs. It is therefore likely that this form is enzymatically active *in vivo*, however the altered spacing between motifs could affect activity. The enzymatic activity of murine *Dnmt3b3* *in vitro* was not addressed in a previous study (27). Preliminary experiments in which the murine *Dnmt3a*, *3b1* and *3b2* cDNAs were transfected into insect cells have confirmed the results of Okano *et al.* that the expressed proteins are enzymatically active using a poly(dI-dC:dI-dC) substrate incubated with cell extracts (P.Vollmayr and N.Reich, personal communication). This, combined with the very high level of homology between the human and murine forms (~95% identity at the amino acid level for *DNMT3a* for example; data not shown) makes it likely that the human forms will possess enzymatic activities similar to the murine homologs. The finding that two of the human splice variants (*DNMT3b4* and *3b5*) result in frameshifts that truncate the protein and delete conserved methyltransferase motifs IX and X may indicate that these forms have differential methylation activities. Interestingly, motifs IX and X, which may be involved in cofactor binding, are not conserved in all known cytosine 5-methyltransferases (11,44). Alternative splicing and differential activity of *DNMT3b* variants could have important implications for cancer. In general it has been observed that bulk DNA becomes hypomethylated in cancer while CpG islands associated with promoters become abnormally *de novo* methylated (6,23). Different forms of the same enzyme, in this case *DNMT3b*, may have enhanced or reduced catalytic activity or may have altered target site specificity (11). An alternatively spliced form with greater affinity for CpG islands or a form which lacks a region preventing its association with CpG islands could help explain the methylation abnormalities associated with cancer. *In vitro* functional studies of the human splice variants will be the subject of future study.

Relating DNMT levels to proliferative state has been an important issue to those studying the role of DNA methylation in cancer. Our studies on the levels of expression of the three DNMT transcripts in normal tissues is, to our knowledge, the most extensive to date and raises several interesting issues. The first relates to the relative levels of the three DNMTs. It was clear, based on exposure times of the northern blots, that *DNMT1* was expressed at the highest level of all three DNMTs in all the normal tissues we examined. The second issue is that, although some relationship between DNMT mRNA levels and proliferative state of the tissue was observed, as evidenced by high level expression in most fetal tissues and adult tissues containing continuously renewing cell populations, such as the thymus, other tissues generally regarded as containing mostly differentiated cells in G₀, such as heart, skeletal muscle, kidney and liver, also contain DNMT levels readily detectable by northern blotting. This may indicate that there are additional levels of control imposed on these enzymes. Additional controls at the level of translational initiation, protein stability and nuclear or cytoplasmic sequestration may be operational. Sequestration of *Dnmt1* in the oocyte cytoplasm has been observed previously (34). Such studies of *DNMT3a* and *3b* will be carried out once antibodies become available and will be an important issue when considering their involvement in cancer as well.

ACKNOWLEDGEMENTS

This work was supported by NIH grant R35 CA 49758 (P.A.J.). K.D.R. was supported by an American Cancer Society post-doctoral fellowship.

REFERENCES

- Bird, A. (1992) *Cell*, **70**, 5–8.
- Cooper, D.N. and Krawczak, M. (1989) *Hum. Genet.*, **83**, 181–188.
- Bird, A. (1986) *Nature*, **321**, 209–213.
- Brandeis, M., Frank, D., Keshet, I., Siegfried, Z., Mendelsohn, M., Nemes, A., Temper, V., Razin, A. and Cedar, H. (1994) *Nature*, **371**, 435–438.
- Macleod, D., Charlton, J., Mullins, J. and Bird, A.P. (1994) *Genes Dev.*, **8**, 2282–2292.
- Jones, P.A. (1996) *Cancer Res.*, **56**, 2463–2467.
- Kass, S.U., Landsberger, N. and Wolffe, A.P. (1997) *Curr. Biol.*, **7**, 157–165.
- Panning, B. and Jaenisch, R. (1998) *Cell*, **93**, 305–308.
- Li, E., Beard, C. and Jaenisch, R. (1993) *Nature*, **366**, 362–365.
- Bestor, T., Laudano, A., Mattaliano, R. and Ingram, V. (1988) *J. Mol. Biol.*, **203**, 971–983.
- Kumar, S., Cheng, X., Klimasauskas, S., Mi, S., Posfai, J., Roberts, R.J. and Wilson, G.G. (1994) *Nucleic Acids Res.*, **22**, 1–10.
- Leonhardt, H., Page, A.W., Weier, H. and Bestor, T.H. (1992) *Cell*, **71**, 865–873.
- Chuang, L.S.-H., Ian, H.-I., Koh, T.-W., Ng, H.-H., Xu, G. and Li, B.F.L. (1997) *Science*, **277**, 1996–2000.
- Li, E., Bestor, T.H. and Jaenisch, R. (1992) *Cell*, **69**, 915–926.
- Walsh, C.P., Chaillet, J.R. and Bestor, T.H. (1998) *Nature Genet.*, **20**, 116–117.
- Lei, H., Oh, S.P., Okano, M., Juttermann, R., Goss, K.A., Jaenisch, R. and Li, E. (1996) *Development*, **122**, 3195–3205.
- Pradhan, S., Talbot, D., Sha, M., Benner, J., Hornstra, L., Li, E., Yaenisch, R. and Roberts, R.J. (1997) *Nucleic Acids Res.*, **25**, 4666–4673.
- Bestor, T.H. (1992) *EMBO J.*, **11**, 2611–2617.
- Vertino, P.M., Yen, R.-W.C., Gao, J. and Baylin, S.B. (1996) *Mol. Cell. Biol.*, **16**, 4555–4565.
- Wu, J., Issa, J.P., Herman, J., Bassett, D.E., Nelkin, B.D. and Baylin, S.B. (1993) *Proc. Natl Acad. Sci. USA*, **90**, 8891–8895.
- Kautiainen, T.L. and Jones, P.A. (1986) *J. Biol. Chem.*, **261**, 1294–1598.
- Issa, J.-P., Vertino, P.M., Wu, J., Sazawal, S., Celano, P., Nelkin, B.D., Hamilton, S.R. and Baylin, S.B. (1993) *J. Natl Cancer Inst.*, **85**, 1235–1240.
- Feinberg, A.P., Gehrke, C.W., Kuo, K.C. and Ehrlich, M. (1988) *Cancer Res.*, **48**, 1159–1161.
- Lee, P.J., Washer, L.L., Law, D.J., Boland, C.R., Horon, I.L. and Feinberg, A.P. (1996) *Proc. Natl Acad. Sci. USA*, **93**, 10366–10370.
- Yoder, J.A. and Bestor, T.H. (1998) *Hum. Mol. Genet.*, **7**, 279–284.
- Okano, M., Xie, S. and Li, E. (1998) *Nucleic Acids Res.*, **26**, 2536–2540.
- Okano, M., Xie, S. and Li, E. (1998) *Nature Genet.*, **19**, 219–220.
- Gonzalzo, M.L., Hayashida, T., Bender, C.M., Pao, M.M., Tsai, Y.C., Gonzales, F.A., Nguyen, H.D., Nguyen, T.-D. and Jones, P.A. (1998) *Cancer Res.*, **58**, 1245–1252.
- Robertson, K.D. and Jones, P.A. (1998) *Mol. Cell. Biol.*, **18**, 6457–6473.
- Yen, R.-W.C., Vertino, P.M., Nelkin, B.D., Yu, J.J., El-Deiry, W., Cumaraswamy, A., Lennon, G.G., Trask, B.J., Celano, P. and Baylin, S.B. (1992) *Nucleic Acids Res.*, **20**, 2287–2291.
- Lanyi, A., Li, B., Li, S., Talmadge, C.B., Brichacek, B., Davis, J.R., Kozel, B.A., Trask, B., van den Engh, G., Uzvolgyi, E., Stanbridge, E.J., Nelson, D.L., Chinault, C., Heslop, H., Gross, T.G., Seemayer, T.A., Klein, G., Purtilo, D.T. and Sumegi, J. (1997) *Genomics*, **39**, 55–65.
- Weiss, L. (1988) In Weiss, L. (ed.), *Cell and Tissue Biology. A Textbook of Histology*, 6th Edn. Urban Schwarzenberg, Baltimore, MD.
- Deng, J. and Szyf, M. (1998) *J. Biol. Chem.*, **273**, 22869–22872.
- Mertineit, C., Yoder, J.A., Taketo, T., Laird, D.W., Trasler, J.M. and Bestor, T.H. (1998) *Development*, **125**, 889–897.
- Krishna, T.S.R., Kong, X.-P., Gary, S., Burgers, P.M. and Kuriyan, J. (1994) *Cell*, **79**, 1233–1243.
- Bravo, R. and Macdonald-Bravo, H. (1984) *EMBO J.*, **3**, 3177–3181.
- Morris, G.F. and Mathews, M.B. (1989) *J. Biol. Chem.*, **264**, 13856–13864.
- Szyf, M., Bozovic, V. and Tanigawa, G. (1991) *J. Biol. Chem.*, **266**, 10027–10030.
- Werner, C.A., Dohner, H., Joos, S., Trumper, L.H., Baudis, M., Barth, T.F.E., Ott, G., Moller, P., Lichter, P. and Bentz, M. (1997) *Am. J. Pathol.*, **151**, 335–342.
- Plantaz, D., Mohapatra, G., Matthay, K.K., Pellarin, M., Seeger, R.C. and Feuerstein, G.G. (1997) *Am. J. Pathol.*, **150**, 81–89.
- Park, J.P., Curran, M.J., Levy, N.B., Davis, T.H., Elliot, J.H. and Mohandas, T.K. (1997) *Cancer Genet. Cytogenet.*, **96**, 118–122.
- Wang, P.W., Iannantuoni, K., Davis, E.M., Espinosa, R., Stoffel, M. and LeBeau, M.M. (1998) *Genes Chromosom. Cancer*, **21**, 75–81.
- Nacheva, E., Holloway, T., Carter, N., Grace, C., White, N. and Green, A.R. (1995) *Cancer Genet. Cytogenet.*, **80**, 87–94.
- Klimasauskas, S., Kumar, S., Roberts, R.J. and Cheng, X. (1994) *Cell*, **76**, 357–369.
- Kafri, T., Gao, X. and Razin, A. (1993) *Proc. Natl Acad. Sci. USA*, **90**, 10558–10562.
- Kafri, T., Ariel, M., Brandeis, M., Shemer, R., Urven, L., McCarrey, J., Cedar, H. and Razin, A. (1992) *Genes Dev.*, **6**, 705–714.